Engineering Journal issn: 0125-8281

Article

A Parametric Study of the Insulation Thickness and the Emissivity of the Reflector during the Billet Transport

Chittin Tangthieng* **and Pavorn Supachaipanichpong**

Department of Mechanical Engineering, Faculty of Engineering, Chulalongkorn University, Phayathai Rd., Wangmai, Pathumwan, Bangkok 10330, Thailand
*E-mail: QED690@yahoo.com (Corresponding author)

Abstract. An investigation of the effect of the insulation thickness and the emissivity of the stainless steel reflector of the covering material during the billet transport on the amount of saving energy is presented. A mathematical model of the heat transfer from the billet through the covering material to the environment is developed. The fully implicit scheme of finite difference equations is employed. The numerical solution is obtained by using the linearization technique. The results are presented in terms of a parametric study of the average temperature of the billet and the amount of saving energy. The data from field measurement is used to verify the numerical result in case of the billet transport without the covering material. A good agreement is observed between those two. As the insulation thickness increases, the temperature drop of the billet during the transport decreases due to the lower heat loss to the environment. This result leads to increasing of the amount of saving energy increases from 219.7 to 272.5 MJ as the insulation thickness increases from 12.5 to 50 mm. As the emissivity of the stainless steel reflector increases, the temperature drop of the billet during the transport increases, corresponding to the decreasing amount of saving energy. In case of the 12.5-mm insulation thickness, the effect of the emissivity on both temperature drop and the amount of saving energy is observed when the emissivity is lower than 0.3. The effect of the emissivity on those two is less significant when the insulation thickness reaches 50 mm. The amount of energy saving is approximately 273 MJ regardless of the emissivity of the stainless steel reflector.

Keywords: Parametric study, billet transport, energy saving, iron and steel industry.

ENGINEERING JOURNAL Volume 26 Issue 7
Received 9 March 2022
Accepted 18 July 2022
Published 31 July 2022
Online at https://engj.org/
DOI:10.4186/ej.2022.26.7.13

DOI:10.4186/ej.2022.26.7.13

Nomenclature

A	area, m^2
Bi	Biot number
C	constant
c	specific heat, J/kg K
D	diameter, m
E	energy, J or MJ
F	view factor
g	gravitational acceleration, m/s^2
Fo	Fourier number
h	heat transfer coefficient, W/m^2 K
J	radiosity, W/m^2
k	thermal conductivity, W/m K
L	thickness, m
m, n	finite difference indices
Nu	Nusselt number
Pr	Prandtl number
Q	heat transfer rate, W
Ra	Rayleigh number
Re	Reynold number
T	temperature, K
t	time, s
V	volume, m^3
v	velocity, m/s
x, y	Cartesian coordinates
α	thermal diffusivity, m^2/s
β	thermal expansion coefficient, 1/K
ε	emissivity
ν	kinematic viscosity, m^2/s
ρ	density, kg/m^3
σ	Stefan-Boltzmann constant, W/m^2 K^4

Subscripts

a	air
b	billet
cm	ceramic fiber
$cond$	conduction
$conv$	forced convection
$free$	free convection
gp	gap
i	element
in	inner surface
rad	radiation
s	covering material
st	stainless steel
tot	total
∞	ambient

1. Introduction

The 20-year energy efficiency developed plan from 2011 to 2030 has been developed to provide the national framework on the long-term energy conservation implementation. The national target is to reduce the final energy consumption by 20 percent or approximately 30,000 ktoe by 2030 [1]. The industrial sector contributes by approximately one third of this amount. Base on the energy demand prediction, the basic metal industry is ranked in sixth of the highest energy consumption industries in Thailand with the energy saving potential of 300 ktoe by 2030 [2]. Thus, the energy saving program will be extensively implemented to the iron and steel industry to achieve the target of this energy consumption reduction. In the iron and streel industry, the energy saving program can be categorized by the production processes such as steel making process, casting process, shaping process. This study focuses on the transport between the casting and shaping processes. After the molten steel has been casted through the continuous casting machine, it is solidified and cast into a semi-finished product, namely a billet. It is conveyed to the reheating furnace before being sent to the rolling mill for shaping as shown in Fig. 1. If heat loss during the billet transport is prevented, the energy saving can be achieved by reducing the thermal energy consumption of the reheating furnace. This energy efficiency improvement is usually referred to as the hot charging process [3-4]. Therefore, the prediction of the temperature profile of the billet during the transport is the key for the assessment of this energy saving program.

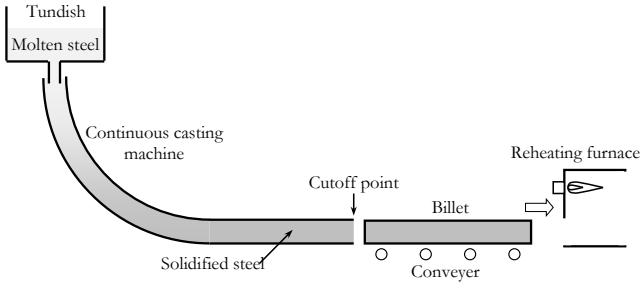

Fig. 1. A diagram of a conveyed billet from the continuous casting machine to the reheating furnace.

In order to predict the billet temperature distribution, the heat conduction models for different processes from the continuous casting process to the rolling mill have been studied. The solidification models for the molten steel during the casting process were developed [5-7]. The heat transfer characteristics including billet conduction, flue gas convection, flue gas radiation, radiation between wall surfaces, and flame combustion, for different types of the reheating furnace, such as pusher-type [8], walking-hearth [9-10], and walking-beam [11-12] one were investigated. The heat conduction models during the billet transport between the reheating furnace and the rolling mill were presented [13-14]. Once the billet temperature distribution was estimated, the amount of the saving energy could be determined. The potential of the energy saving [15] and the economical aspect from the hot charging process were presented [16].

In general, the billet is conveyed without a covering insulation material if the casting machine is located near the reheating furnace. However, the distance between

these two is quite far in many cases, leading to the implementation of the covering material. In addition, the effect of some parameters of the covering material should be further investigated. The aim of this present study is to investigate the energy saving opportunity by applying the insulation box during the biller transport from the continuous casting machine to the reheating furnace. A numerical model of the billet heat conduction and the radiation exchange between surfaces is developed and solved using the finite difference technique. Parametric studies of the insulation thickness and the emissivity of the reflector are performed. The amount of energy saving from the insulation based on these parametric studies is predicted.

2. Problem Formulation

A mathematical model of a billet under consideration is developed first. The billet is made of steel with a square cross-sectional area (A_b) of 130 mm x 130 mm and a length (L_b) of 6 m. In this study, two cases are considered: case (a) the billet transport without the covering material and case (b) the billet transport with the covering material as shown in Fig 2. To simplify the complexity of the billet bottom surface where it is placed on the roller with intermittent gaps, it is assumed that the covering material covers all four billet surfaces. The covering material consists of a layer of ceramic fiber inserted between two stainless steel sheets served as reflectors as illustrated in Fig. 3.

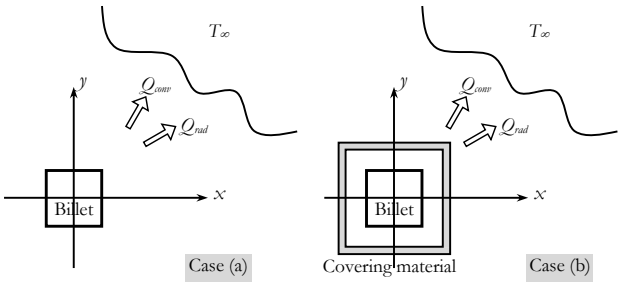

Fig. 2. Two cases under consideration (a) without the covering material and (b) with the covering material.

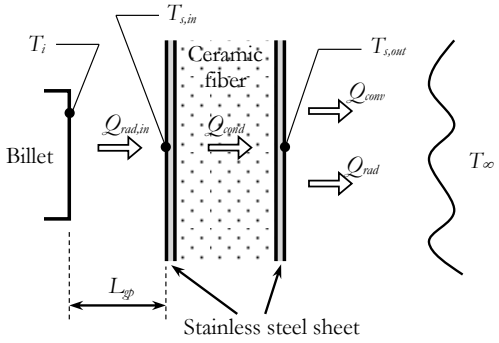

Fig. 3. Component and heat transfer characteristics of the covering material.

The two-dimensional transient heat conduction equation or Eq. (1) for the billet as a system under consideration can be written as

$$\rho_b\, c_b \frac{\partial T}{\partial t} = k_b \left(\frac{\partial^2 T}{\partial x^2} + \frac{\partial^2 T}{\partial y^2} \right) \tag{1}$$

The associated boundary conditions are given by the total heat loss at the billet surfaces (Q_{tot}), which is a combination of the convective heat losses (Q_{conv}) and radiative heat losses (Q_{rad}) as shown in Eq. (2).

$$Q_{tot} = Q_{conv} + Q_{rad} \tag{2}$$

The convective heat loss originated from the motion of the billet in the longitudinal direction through the conveyor at the average conveying speed (v_b) of 1.5 m/s can be expressed as Eq. (3). The average convective heat transfer coefficient (h_{conv}) can be written as Eq. (4) [17].

$$Q_{conv} = h_{conv} A_i \left(T_i - T_\infty \right) \tag{3}$$

$$\begin{aligned} Nu_L &= \frac{h_{conv} L_b}{k_a} = 0.664\, Re_L^{0.5} Pr^{1/3} \\ &= 0.664 \left(\frac{v_b L_b}{\nu_a} \right)^{0.5} \left(\frac{\rho_a \nu_a c_a}{k_a} \right)^{1/3} \end{aligned} \tag{4}$$

The radiative heat loss from the billet surface from each case is different as follows:

(i) Case (a): without the covering material

With the absence of the covering material, the radiative heat loss from the billet directly to the environment can be linearized and written in terms of the radiative heat transfer coefficient (h_{rad}) as shown in Eqs. (5) and (6).

$$Q_{rad} = \varepsilon\sigma A_i \left(T_i^4 - T_\infty^4 \right) = h_{rad} A_i \left(T_i - T_\infty \right) \tag{5}$$

$$h_{rad} = \varepsilon\sigma \left(T_i + T_\infty \right) \left(T_i^2 + T_\infty^2 \right) \tag{6}$$

(ii) Case (b): with the covering material

The radiation exchange between the billet surfaces and the inner surface of the covering material made of stainless steel can be assumed to be the radiation exchange between two diffused, grey surfaces. For simplicity, the temperature of the covering material is uniform throughout its perimeter. Because the finite different discretization will later be employed to solve the temperature distribution of the billet, the covering material will be served as an enclosure for each element of the billet surface. Under this configuration, the view factor of each billet element to the enclosure (F_{is}) is unity. The net rate of total radiation transfer from all elements

of the billet surface ($Q_{rad,in,tot}$) to the inner surface of the covering material is given by Eq. (7) [18].

$$Q_{rad,in,tot} = \sum_i \frac{\sigma T_i^4 - J_s}{\frac{1-\varepsilon_i}{\varepsilon_i A_i} + \frac{1}{A_i F_{is}}} = \frac{J_s - \sigma T_s^4}{\frac{1-\varepsilon_s}{\varepsilon_s A_s}} \tag{7}$$

To utilize the radiative heat transfer coefficient concept similar to Eq. (5), the radiosity of the covering material surface (J_s) shown in Eq. (7) is eliminated. The net rate of radiation transfer from each element of the billet surface ($Q_{rad,in}$) can be expressed in terms of $h_{rad,in}$ as shown in Eq. (8). This radiative heat transfer concept will be beneficial for the number solution procedure described later in Section 4.

$$Q_{rad,in} = \frac{\sigma\left(T_i^4 - T_{si}^4\right)}{\frac{1}{\varepsilon_i A_i} + \frac{1-\varepsilon_s}{\varepsilon_s A_{si}}} = h_{rad,in} A_i \left(T_i - T_{si}\right) \tag{8}$$

Heat conduction (Q_{cond}) from the inner surface of the covering material through insulation layers to the environment is assumed one dimensional and quasi steady. Heat is conducted through the covering material, and transferred out to the environment by the free convection and radiation as shown in Fig. 3. Both can be described by Eqs. (9) and (10).

$$Q_{cond} = \frac{T_{s,in} - T_{s,out}}{2\frac{L_{st}}{k_{st} A_s} + \frac{L_{cm}}{k_{cm} A_s}} \tag{9}$$

$$Q_{free} + Q_{rad} = h_{free}\left(T_{s,out} - T_\infty\right) + \varepsilon\sigma\left(T_{s,out}^4 - T_\infty^4\right) \tag{10}$$

In case of the free convection at the outer surface of the covering material to the environment, the convective heat transfer coefficient (h_{free}) for a long horizontal cylinder can be determined by the correlation of Morgan or Eq. (11) with C = 0.125 and n = 0.333 [19]. The diameter of the cylinder is replaced by the hydraulic diameter (D_h) of the covering material.

$$Nu_{D_h} = \frac{h_{free} D_h}{k_a} = C\, Ra_{D_h}^n = C\left(\frac{g\,\beta_a\,\Delta T\, D_h^3}{\nu_a\,\alpha_a}\right)^n \tag{11}$$

3. Finite Difference Approximation

The physical system governed by the heat conduction equation or Eq. (1) is discretized into orthogonal grids with the grid size of Δx and Δy. Because of the billet with a square cross section, Δx and Δy is identical. The finite difference approximation for each node $T^p_{m,n}$ in both x and y directions is related to the adjacent nodes as shown in Fig. 4.

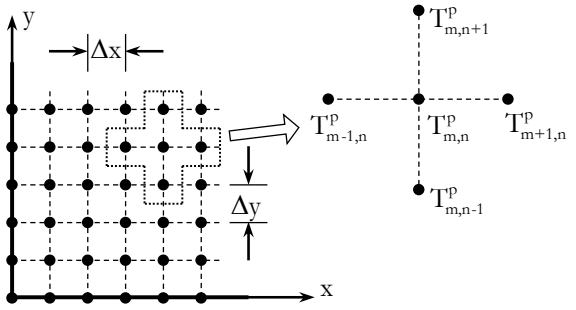

Fig. 4. A schematic of grid arrangement.

In addition, the fully implicit scheme is employed to ensure the unconditional stability for any size of a time step [20]. As a result, the finite different approximations for the time and spatial derivatives in Eq. (1) can be expressed as Eqs. (12) to (14).

$$\frac{\partial T}{\partial t} \approx \frac{T_{m,n}^{P+1} - T_{m,n}^{P}}{\Delta t} \tag{12}$$

$$\frac{\partial^2 T}{\partial x^2} = \frac{T_{m+1,n}^{P+1} - 2T_{m,n}^{P+1} + T_{m-1,n}^{P+1}}{\left(\Delta x\right)^2} \tag{13}$$

$$\frac{\partial^2 T}{\partial y^2} = \frac{T_{m,n+1}^{P+1} - 2T_{m,n}^{P+1} + T_{m,n-1}^{P+1}}{\left(\Delta y\right)^2} \tag{14}$$

By substituting Eqs. (12) to (14) into Eq. (1) with further simplification, the finite different equations for an interior node, an edge node, and a corner node can be expressed as Eqs. (15) to (17), respectively.

$$\begin{aligned}&\left(1+4Fo\right)T_{m,n}^{P+1} - Fo\,T_{m+1,n}^{P+1} - Fo\,T_{m-1,n}^{P+1}\\ &-Fo\,T_{m,n+1}^{P+1} - Fo\,T_{m,n-1}^{P+1} \;=\; T_{m,n}^{P}\end{aligned} \tag{15}$$

$$\begin{aligned}&\left(1+2\,Bi\,Fo+4\,Fo\right)T_{m,n}^{P+1} - Fo\,T_{m+1,n}^{P+1}\\ &-Fo\,T_{m-1,n}^{P+1} - 2\,Fo\,T_{m,n+1}^{P+1} \;=\; T_{m,n}^{P} + 2\,Bi\,Fo\,T_\infty\end{aligned} \tag{16}$$

$$\begin{aligned}&\left(1+4\,Bi\,Fo+4\,Fo\right)T_{m,n}^{P+1} - 2\,Fo\,T_{m+1,n}^{P+1}\\ &-2\,Fo\,T_{m-1,n}^{P+1} \;=\; T_{m,n}^{P} + 4\,Bi\,Fo\,T_\infty\end{aligned} \tag{17}$$

The Biot number (Bi) and Fourier number (Fo) are defined by Eq. (18).

$$Bi = \frac{h_{tot}\Delta x}{k_b} \quad \text{and} \quad Fo = \frac{\alpha_b \Delta t}{\left(\Delta x\right)^2} \tag{18}$$

4. Numerical Solution Procedure

In order to initiate the numerical procedure, the initial condition of the billet is set to be 950°C, corresponding to its approximate temperature after the cutoff point shown in Fig. 1 [21]. The ambient temperature (T_∞) is 32°C. For simplicity, the properties

of air appearing in the convective parts are assumed constant and evaluated at the film temperature of 491°C as shown in Table 1 [22]. The thermal expansion coefficient (β) is determined based on the ideal gas assumption for air.

Table 1. Properties of air.

No.	Symbol	Value
1	k_a	0.05558 W/m-K
2	ρ_a	0.4561 kg/m^3
3	c_a	1090 J/kg-K
4	ν_a	7.879x10^{-7} m^2/s
5	β_a	1.309x10^{-3} 1/K

The properties of the billet made of low-carbon steel are provided in Table 2 [23].

Table 2. Dimensions and properties of the steel billet.

No.	Symbol	Value
1	A_b	0.13 m x 0.13 m
2	L_b	6 m
3	k_b	29.4 W/m-K
4	ρ_b	7600 kg/m^3
5	c_b	670 J/kg-K

The emissivity of the steel billet is assumed to be a linear function of its temperature from 380°C to 520°C as shown in Eq. (19) [24].

$$\varepsilon_i = \begin{cases} 0.28 & ; \quad T < 380^o C \\ 0.00304T - 0.888 & ; \quad 380 \le T < 520^o C \\ 0.69 & ; \quad T \ge 520^o C \end{cases} \qquad (19)$$

The dimensions and properties of the covering material made of ceramic fiber and stainless steel sheets are given in Table 3.

Table 3. Dimensions and properties of the covering material.

No.	Symbol	Value
1	k_{cm}	0.11 W/m-K
2	k_{st}	20 W/m-K
3	L_{st}	1 mm
4	L_{gp}	25 mm
5	A_s	4.32 m^2

In this study, the thickness of ceramic fiber and the emissivity of the stainless steel sheet are two of the varying parameters for the energy saving analysis. The thickness of ceramic fiber varies from 12.5 to 50 mm whereas the emissivity of the stainless steel sheet varies from 0.1 to 0.9. The increasing emissivity of the stainless steel sheet originates from the oxidation of the stainless steel surface in case of operating at a high temperature for a long time.

In order to solve for the solution, the MATLAB™ software is applied for numerical computation. Because the system of finite difference equations developed from Eqs. (15) to (17) can be linearized in terms of the radiative heat transfer coefficient, the lagging coefficient technique is employed to overcome the nonlinearity [25-26]. In case of no covering material, h_{rad} can be simply linearized by Eq. (6). On the other hand, in case with the coving material, $T_{s,in}$ from Eq. (9) can be determined based on the billet surface temperature or T_i at the previous time step. The input heat to the covering material from Eq. (7) must be identical to the output heat from the covering material to the environment from Eqs. (9) and (10) according to the heat balance, resulting in the value of $T_{s,in}$. It is noted that the successive iteration method is employed to seek for the solution of $T_{s,in}$. Thereafter, the value of T_i from the next time step will be determined by solving the system of Eqs. (15) to (17) with the lagging coefficient technique to linearize $h_{rad,in}$ from Eq. (8), similar to the case without the covering material.

The grid dependence is first examined by using the different values of uniform grid of sizes 5x5, 10x10, and 20x20. By setting the result from the 20x20 grid as a reference case, the relative errors of the average billet temperature obtained from the 5x5 grid and the 10x10 grid are 0.179 and 0.0229 percent, respectively. Therefore, the uniform grid of size 10x10 with the identical values of Δx and Δy of 13 mm is chosen in this study to keep the relative error less than 0.1 percent. The numerical computation is run on the time step of 1 second until it reaches 3,600 second.

5. Results and Discussion

The numerical result in case of no covering material is verified by the data obtained from the field measurement using a thermal imaging camera. After the billet has been cut to a proper length at the cutoff point, the thermal images with a resolution of 384x288 pixels are captured. The surface temperature obtained by the camera has a range between –40°C to 2000°C with the accuracy of 2 percent of reading. The field data is recorded in every one minute for the record period of one hour. The data from the captured image will be processed through the manufacturer software to obtain the average surface temperature of the billet. It is compared with the result obtained by the numerical prediction as shown in Fig. 5. It can be seen that the average surface temperatures obtained from both numerical prediction and field measurement are in a good agreement. By comparing the results obtained from two approaches, those from the field data are slightly higher than those from the numerical prediction by approximately 9.83 percent.

DOI:10.4186/ej.2022.26.7.13

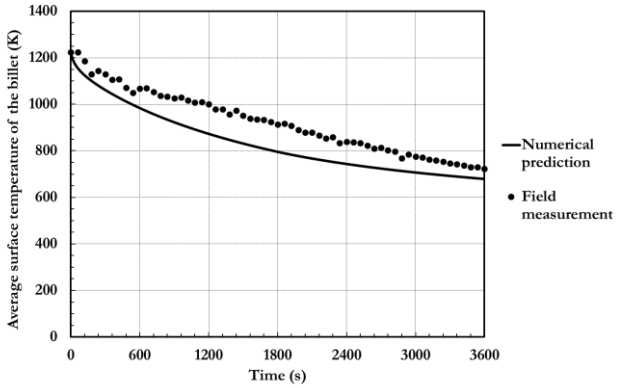

Fig. 5. Comparison of the billet surface temperatures between the numerical prediction and field measurement.

The temperature profiles of the billet from the numerical prediction at different times in case without the covering material are illustrated in Fig. 6. Due to the symmetry along both x and y axes, the temperature starts decreasing from the billet center at x=0 to the minimum value at the billet edge at x=65 mm. After leaving the billet to cool down from the initial temperature of 1223.15 K (950°C), the temperature at the billet center drops rapidly to 1137 K whereas the temperature at the billet edge drops further to 1066 K in 300 s. As the time goes by, the reduction rate of the billet temperature starts declining and the temperature uniformity increases. At the end of the simulation of 3600 s, the temperature at the billet center is 650.6 K whereas the temperature at the billet edge is 641.3 K. This indicates the higher temperature uniformity of the billet compared to that at the early cooling stage.

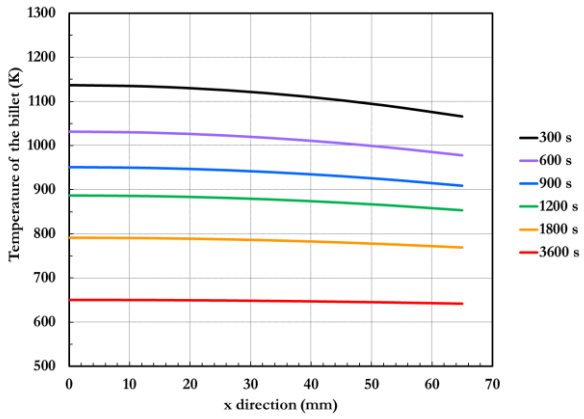

Fig. 6. The temperature profile of the billet in case without the covering material at different times.

In order to determine the amount of the saving energy, the amount of required energy for the billet to reheat back to 1,250°C (T_{reheat}) should be considered first. This energy can be directly calculated from the average billet temperature ($\overline{T}$) as shown in Eq. (20).

$$E_{req} = \rho_b V_b c_b \left(T_{reheat} - \overline{T}\right) \quad (20)$$

The difference between E_{req} from a case under consideration and E_{req} from a reference case represents the amount of the saving energy of that one. In this study, a reference case is the one without the covering material. Then, the parametric study of the insulation thickness and the emissivity of the stainless steel sheet with respect to the average temperature of the billet and the amount of the saving energy will be performed and investigated.

Figures 7 and 8 illustrate the variations of the average temperature of the billet and the amount of saving energy with different insulation thicknesses.

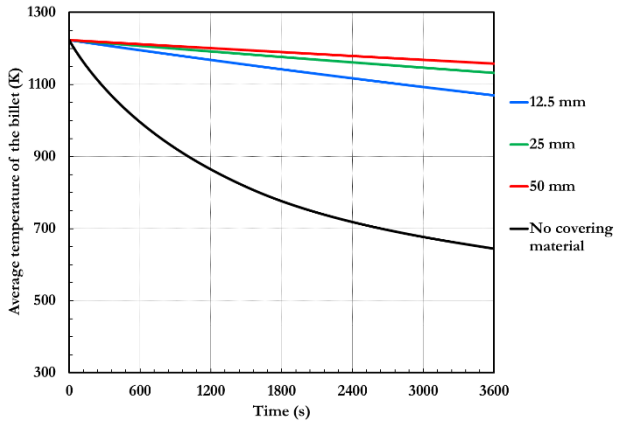

Fig. 7. Variations of the average temperature of the billet with different insulation thicknesses.

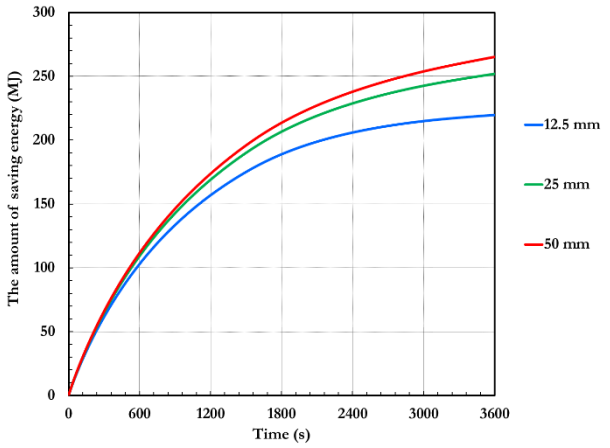

Fig. 8. Variations of the amount of saving energy with different insulation thicknesses.

The emissivity of the stainless steel sheet served as a reflector is set to 0.6 as a baseline case. After an hour of simulation, it can be seen that the final temperature of the billet drops from the initial temperature of 1223.15 K (950°C) to the lowest value of 644.3 K in case of no covering material. On the other hand, when the thermal insulation is used, the final temperatures of the billet do not decrease as much as the case without covering material. The final temperatures of the billet in case of the insulation thickness of 12.5, 25 and 50 mm are 1069.8, 1132.2, and 1172.1 K, respectively. This result

indicates that implementation of the covering material leads to the prevention of the significant amount of heat loss. The amount of saving energy is potentially higher in the case with thicker insulation thickness as expected. At the final time, it reaches the highest values of 219.7, 251.9, and 272.5 MJ for the insulation thickness of 12.5, 25 and 50 mm, respectively. It is noticed that the increasing rate of the saving energy slows down as the insulation gets thicker. This may limit the insulation thickness due to the economical reason.

Figures 9 and 10 depict the variations of the average temperature of the billet and the amount of saving energy with different values of the emissivity of the stainless steel sheet for 12.5-mm insulation thickness.

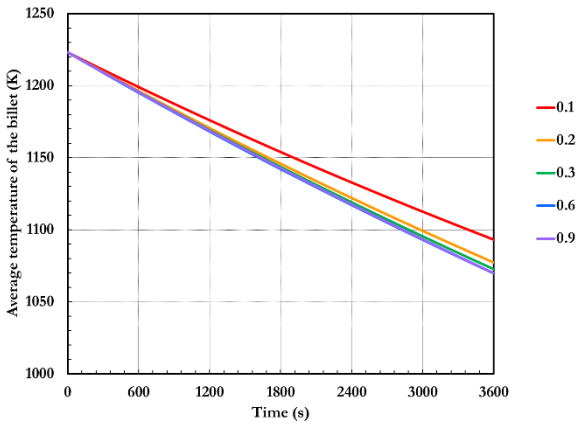

Fig. 9. Variations of the average temperature of the billet with different values of the emissivity of the stainless steel sheet for 12.5-mm insulation thickness.

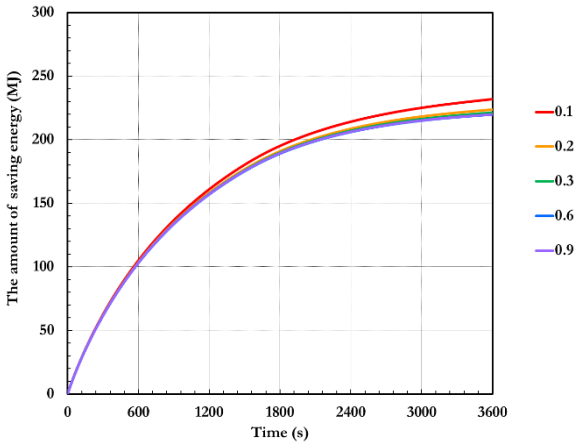

Fig. 10. Variations of the amount of saving energy with different values of the emissivity of the stainless steel sheet for 12.5-mm insulation thickness.

The result indicates that the average billet temperatures at the final time are 1093.2, 1072.7, and 1069.9 K for the emissivity of 0.1, 0.3, and 0.9, respectively, leading to the amount of saving energy of 231.8, 221.2, and 219.8 MJ. As the emissivity increases, the ability to reflect the radiation of the stainless steel reflector deceases causing the higher amount of heat loss through the cover material. As a result, the average billet temperature at the final time will drop further in the case with higher emissivity. However, it is noticed that the changes of the average billet temperature and the amount of saving energy start declining when the emissivity increases above 0.3.

Figures 11 and 12 illustrate the variations of the average temperature of the billet and the amount of saving energy with different values of the emissivity of the stainless steel sheet for 25-mm insulation thickness.

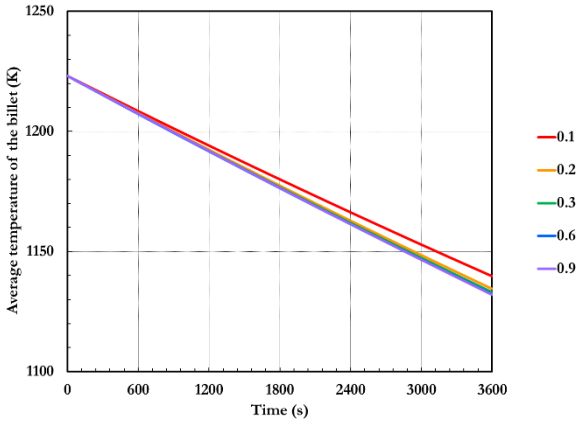

Fig. 11. Variations of the average temperature of the billet with different values of the emissivity of the stainless steel sheet for 25-mm insulation thickness.

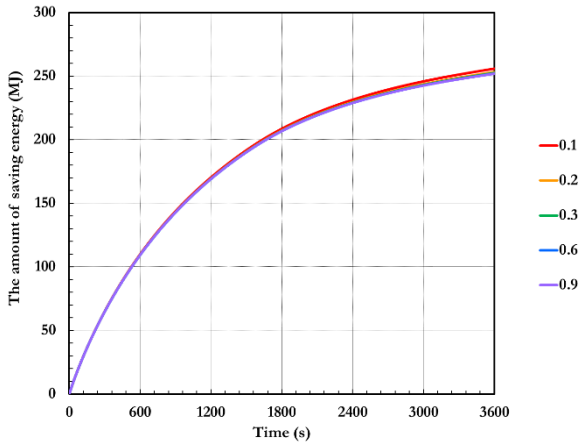

Fig. 12. Variations of the amount of saving energy with different values of the emissivity of the stainless steel sheet for 25-mm insulation thickness.

The average billet temperatures at the final time are 1139.7, 1133.1, and 1132.0 K for the emissivity of 0.1, 0.3, and 0.9, respectively. On the other hand, the amount of saving energy for those three cases is 255.8, 252.3, and 251.8 MJ, respectively. It is noticed that the difference of the saving energy by increasing emissivity from 0.1 to 0.9 is lower comparing to the case of 12.5-mm insulation thickness. When the insulation gets thicker, the heat loss to the environment is mainly controlled by heat conduction through the ceramic fiber.

As a result, the effect of the emissivity of the reflector on the heat loss significantly diminishes.

Figures 13 and 14 depict the variations of the average temperature of the billet and the amount of saving energy with different values of the emissivity of the stainless steel sheet for 50-mm insulation thickness.

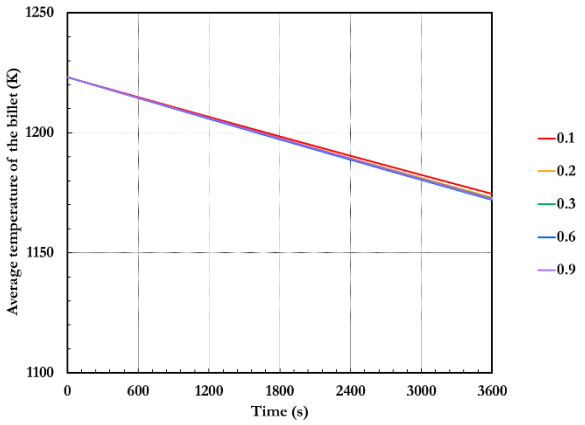

Fig. 13. Variations of the average temperature of the billet with different values of the emissivity of the stainless steel sheet for 50-mm insulation thickness.

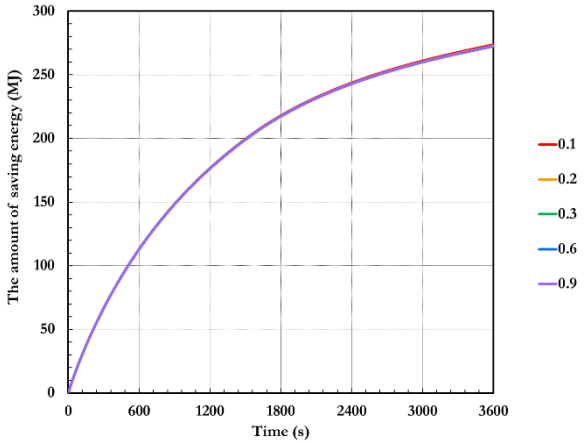

Fig. 14. Variations of the amount of saving energy with different values of the emissivity of the stainless steel sheet for 50-mm insulation thickness.

The results show that the average billet temperatures at the final time are 1174.6, 1172.5, and 1172.1 K for the emissivity of 0.1, 0.3, and 0.9, respectively, leading to the amount of saving energy of 273.8, 272.7, and 272.5 MJ. In this case, the difference of the saving energy by increasing emissivity from 0.1 to 0.9 is very marginal. By comparing with the previous cases, this amount corresponds to 12.0, 4.0, and 1.3 MJ for the insulation thickness of 12.5, 25, and 50 mm, respectively.

6. Conclusion

An investigation of the parametric study of the insulation thickness and the emissivity of the stainless steel reflector of the covering material during the billet transport has been presented in this study. A mathematical model of the billet heat conduction and the radiation exchange between the billet surface and the inner surface of the covering material was developed. The finite difference approximation was employed to solve for the numerical solutions. The average temperature of the billet and the amount of saving energy were the main result for this investigation. The numerical result in case of the billet transport without the covering material was verified by the data from field measurement. A good agreement was observed between those two. The numerical result indicated that as the insulation thickness increases, the amount of heat loss decreases significantly. By comparing to the case without the covering material, the final temperature increased from 1069.8 to 1172.1 K and the amount of saving energy increased from 219.7 to 272.5 MJ as increasing insulation thickness from 12.5 to 50 mm. As the emissivity of the stainless steel reflector increased from 0.1 to 0.9 in case of the 12.5-mm thick insulation, the temperature drop of the billet during the transport increased, corresponding to the decreasing amount of saving energy from 231.8 to 219.8 MJ. In this case, it was also observed that the effect of the emissivity on those two was significant when the emissivity was lower than 0.3. On the other hand, the effect of the emissivity on those two was less significant as the insulation gets thicker. When the insulation thickness was 50 mm, the amount of energy saving was approximately 273 MJ regardless of the emissivity of the reflector. It is suggested that the economical aspect of the proper insulation thickness relevant to the conveying distance should be further studied.

Acknowledgement

The authors greatly acknowledge the Iron and Steel Institute of Thailand (ISIT) through the project entitled "Improvement of energy efficiency in the iron and steel industry by hot charging process", 2017.

References

[1] Ministry of Energy. (2011). Thailand 20-Year Energy Efficiency Development Plan or EEDP (2011-2030). [Online]. Available: http://www.eppo.go.th/images/POLICY/ENG/EEDP_Eng.pdf [Accessed: 29 January 2022].

[2] A. Chaichaloempreecha, P. Winyuchakrit, and B. Limmeechokchai, "Assessment of renewable energy and energy efficiency plans in Thailand's industrial sector," *Energy Procedia*, vol. 138, pp. 841-846, 2017.

[3] H. Na, J. Sun, Z. Qiu, J. He, Y. Yuan, T. Yan, and T. Du, "A novel evaluation method for energy efficiency of process industry—A case study of typical iron and steel manufacturing process," *Energy*, vol. 233, 2021, Art. no. 121081.

[4] J. Zhao, L. Ma, M. E. Zayed, A. H. Elsheikh, W. Li, Q. Yan, and J. Wang, "Industrial reheating furnaces: A review of energy efficiency assessments, waste

heat recovery potentials, heating process characteristics and perspectives for steel industry," *Process Safety and Environmental Protection*, vol. 147, pp. 1209-1228, 2021.

[5] A. Ramírez-López, R. Aguilar-López, M. Palomar-Pardavé, M. A. Romero-Romo, and D. Muñoz-Negrón, "Simulation of heat transfer in steel billets during continuous casting," *International Journal of Minerals, Metallurgy and Materials*, vol. 17, no. 4, pp. 403-414, 2010.

[6] A. Ramírez-López, O. Dávila-Maldonado, A. Nájera-Bastida, R. D. Morales, J. Rodríguez-Ávila, and C. R. Muñiz-Valdés, "Analysis of non-symmetrical heat transfers during the casting of steel billets and slabs. *Metals*, vol. 11, no. 9, pp. 1380, 2021.

[7] V. I. Odinokov, A. I. Evstigneev, and E. A. Dmitriev, "Numerical simulation of metal filling into a CCM mold equipped with a deflector,". *Steel in Translation*, vol. 49, no. 10, pp. 653-660, 2019.

[8] T. Khoukit and C. Tangthieng, "A numerical investigation of the temperature uniformity of a billet due to thermal radiation in a reheating furnace," *Engineering Journal*, vol. 20, no. 1, pp. 35-46, 2016.

[9] R. Prieler, B. Mayr, M. Demuth, B. Holleis, and C. Hochenauer, "Prediction of the heating characteristic of billets in a walking hearth type reheating furnace using CFD," *International Journal of Heat and Mass Transfer*, vol. 92, pp. 675-688, 2016.

[10] A. Emadi, A. Saboonchi, M. Taheri, and S. Hassanpour, "Heating characteristics of billet in a walking hearth type reheating furnace," *Applied Thermal Engineering*, vol. 63, no. 1, pp. 396-405, 2014.

[11] S. K. Dubey and P. Srinivasan,"Development of three dimensional transient numerical heat conduction model with growth of oxide scale for steel billet reheat simulation," *International Journal of Thermal Sciences*, vol. 84, pp. 214-227, 2014.

[12] A. M. García and A. A. Amell, "A numerical analysis of the effect of heat recovery burners on the heat transfer and billet heating characteristics in a walking-beam type reheating furnace," *International Journal of Heat and Mass Transfer*, vol. 127, pp. 1208-1222, 2018,

[13] A. Jaklič, B. Glogovac, T. Kolenko, B., Zupančič, and B. Težak, "A simulation of heat transfer during billet transport," *Applied Thermal Engineering*, vol. 22, no. 7, pp. 873-883, 2002.

[14] K. N. Cançado, L. Machado, and L. N. Soares, "Analysis of heat transfer in steel billets during transport," *Revista de Engenharia Térmica*, vol. 17, no. 1, pp. 69-72, 2018.

[15] S. V. Lukin, A. A. Zbrodov, and K. Y. Levashev, "Hot-slab charging for energy conservation in continuous furnaces," *Metallurgist*, vol. 64, no. 7, pp. 605-614, 2020.

[16] D. L. Jones, "Available and emerging technologies for reducing greenhouse gas emissions from the iron and steel industry," US EPA, Office of Air Quality Planning and Standards, Sector Policies and Programs Division, pp. 25, 2012.

[17] Y. Cengel, "External forced convection," in *Heat and Mass Transfer: A Practical Approach*, 3rd ed. Singapore: McGraw Hill, 2006, ch. 7, sec. 7-2, pp. 401-403.

[18] M. N. Özışık, "Radiation among surfaces in a nonparticipating medium," in *Heat Transfer: A Basic Approach*. Singapore: McGraw Hill, 1985, ch. 12, sec. 12-10, pp. 657-666.

[19] V. T. Morgan, "The overall convective heat transfer from smooth circular cylinders," *Advances in Heat Transfer*, vol. 11, pp. 199-264, 1975.

[20] S. C. Chapra and R. P. Canale, "A simple implicit method," in *Numerical Methods for Engineers*, 6th ed. New York: McGraw Hill, 2010, ch. 30, sec 30.3, pp. 876-880.

[21] C. A. Santos, A. Garcia, A., C. R. Frick, and J. A. Spim, "Evaluation of heat transfer coefficients along the secondary cooling zones in the continuous casting of steel billets," *Inverse Problems in Science and Engineering*, vol. 14, no. 6, pp. 687-700, 2006.

[22] F. P. Incropera, D. P. DeWitt, T. L. Bergman, and A. S. Lavine, "Thermophysical properties of matter," in *Fundamentals of Heat and Mass Transfer*, 6th ed. Singapore: John Wiley & Sons, 2007, appendix A, sec. A.4, pp. 941.

[23] M. Jiaocheng, L. Jun, Y. Qiang, and C. Liangyu, "The temperature field measurement of billet based on multi-information fusion," *Materials Transactions*, vol. 55, no. 8, pp. 1319-1323, 2014.

[24] H. Sadiq, M. B. Wong, J. Tashan, R. Al-Mahaidi, and X. L. Zhao, "Determination of steel emissivity for the temperature prediction of structural steel members in fire," *Journal of Materials in Civil Engineering*, vol. 25, no. 2, pp. 167-173, 2013.

[25] S. V. Patankar, "Steady one dimensional conduction," in *Numerical Heat Transfer and Fluid Flow*. Taylor & Francis, 1980, ch 4, sec. 4.2-4, pp. 47-48.

[26] G. C. Bourantas and V. N. Burganos, "An implicit meshless scheme for the solution of transient non-linear Poisson-type equations," *Engineering Analysis with Boundary Elements*, vol. 37, no. 7-8, pp. 1117-1126, 2013.

DOI:10.4186/ej.2022.26.7.13

Chittin Tangthieng was born in Bangkok, Thailand. He received the B.Eng. degree in mechanical engineering from Chulalongkorn Universiry, Thailand, in 1994. He completed his master degree in mechanical engineeering from University of Washington, Seattle, WA, USA, in 1998, and earned his Ph.D. in mechanical engineering from the Pennslyvania State University, State College, PA, USA, in 2002. He is currently an associate professor in the department of mechanical engineering, Chulalongkorn University. His research interests include energy management in buildings, energy efficiency in an iron and steel industry, refrigeration and air conditioning, and modeling and simulation of thermal power plants

Pavorn Supachaipanichpong was born in Rachaburi, Thailand. He received the B.Eng. and M.S. degrees in mechanical engineering from Chulalongkorn University, Thailand, in 2016 and 2019, respectively.